Proceedings of the 5th International Conference on Biological Engineering and Medical Science
DOI: 10.54254/2753-8818/99/2025.23533

Cell Membrane-Encapsulated Biomimetic Nanomedicines Carrying siRNA for Glioblastoma Treatment via Gene Silencing Synergistic Phototherapy

Lingchuan Wang

The Village School, Houston, USA
Lingchuanwangyyds@gmail.com

Abstract: The synergy between phototherapy and gene therapy, which relies on photothermal promotion of siRNA release to achieve regulation of RNA interference genes, has resulted in excellent synergy and high efficacy of combined phototherapy-gene therapy, which has shown great potential in tumor therapy. Here, we synthesized gold nanomaterials (Au NRs) with near-infrared absorption and piggybacked Bcl-2 siRNAs (Bcl-2@Au NPs) on their surfaces using a silver (Ag) template method. In addition, the tumor cell membrane (CM) was modified on the surface to consider the effect of the blood-brain barrier in the brain, which resulted in a higher targeting ability of Bcl-2@Au NPs -CM to the glioblastoma region. Under the irradiation of NIR light, the temperature of Bcl-2@Au NPs-CM accumulated at the tumor site increased to induce apoptosis in tumor cells. The main function of Bcl-2 as an apoptosis inhibitory protein is to protect cells from apoptosis by inhibiting the activity of apoptotic factors, which would hinder the effect of phototherapy on tumor cells. However, Bcl-2 siRNA released from Bcl-2@Au-CM NPs in tumor cells inhibits the overexpression of Bcl-2 in the cytoplasm, which would exacerbate the apoptotic effect of phototherapy. Therefore, the anti-tumor efficacy of the administration therapy of Bcl-2@Au-CM NPs was significantly improved due to the efficient synergistic delivery ability of phototherapy-gene therapy. Phototherapy and gene therapy are synergistic and mutually reinforcing, and have excellent prospects for clinical application in the field of tumor therapy.

Keywords: phototherapy, gene therapy, tumor therapy

1. Introduction

Gliomas are common primary tumors of the central nervous system that are difficult to treat and have a poor prognosis [1]. Current treatments mainly include surgery, radiation and chemotherapy with limited results [2]. Conventional therapies often have serious side effects and may not reach all cancer cells hidden in the brain, largely due to the protection of a tight barrier known as the blood-brain barrier (BBB) [3, 4]. Surgery is the treatment of choice for gliomas, with the goal of removing as much of the tumor as possible, relieving symptoms and setting the stage for subsequent treatment. However, due to the infiltrative growth of the tumor and the unclear border with normal brain tissue, complete removal is difficult and prone to recurrence. Radiation therapy is often used as an adjuvant treatment after surgery or for patients who cannot undergo surgery [5]. It kills tumor cells through high-energy radiation, but it also damages normal brain tissue and causes side effects. Chemotherapy

© 2025 The Authors. This is an open access article distributed under the terms of the Creative Commons Attribution License 4.0 (https://creativecommons.org/licenses/by/4.0/).

DOI: 10.54254/2753-8818/99/2025.23533

uses drugs to kill tumor cells, and commonly used drugs include temozolomide (TMZ) [6]. However, chemotherapy drugs have difficulty crossing the blood-brain barrier and are prone to drug resistance, resulting in limited efficacy. Despite the variety of treatments available, the prognosis for gliomas, particularly high-grade gliomas such as glioblastoma, remains poor. Current research is focused on developing new targeted agents, immunotherapies, and combination therapies to improve efficacy and quality of life for patients [7].

Photothermal therapy (PTT) is a treatment method that uses a photothermal converter to convert light energy into heat energy to kill tumor cells by local heating [8, 9]. Compared to traditional therapies, PTT has the advantages of being minimally invasive, precise, and with fewer side effects [10]. However, traditional photothermal converters have problems such as low photothermal conversion efficiency, poor targeting, and insufficient biocompatibility, which limit their clinical applications. At the same time, the higher temperature inside the tumor cells causes the cells to activate self-protection mechanisms that prevent apoptosis. Nanomaterial photothermal therapy for tumor treatment provides new ideas. Nanomaterial photothermal therapy uses nanomaterials as photothermal conversion agents, which has the following advantages High efficiency of photothermal conversion: Nanomaterials such as gold nanorods, copper sulfide and other nanomaterials have excellent photothermal conversion efficiency, which can efficiently convert light energy into heat energy [11]. Precise targeting: Nanomaterials can precisely identify tumor cells by surface modification of targeting molecules, which can improve therapeutic effect and reduce side effects. Multifunctionality: Nanomaterials can integrate diagnostic and therapeutic functions to realize integrated diagnosis and treatment [12, 13]. Combined therapy: Nanomaterials can be loaded with chemotherapeutic drugs, protein inhibitors, etc., to realize synergistic treatment between photothermal therapy and other therapies and enhance the therapeutic effect [14, 15].

Gene therapy is a method of treating disease by introducing exogenous genes into target cells to correct or compensate for defective genes [16, 17]. It offers new treatment ideas for hereditary diseases, cancer, infectious diseases and other intractable diseases. Gene therapy can directly target the genetic roots of diseases, repair or replace defective genes to achieve fundamental treatment, and the successfully introduced exogenous genes can be expressed in cells for a long time to achieve long-lasting therapeutic effects. Meanwhile, gene therapy has a broad therapeutic scope and can be applied to all diseases caused by genetic abnormalities. Gene delivery is the core of gene therapy, and its goal is to efficiently and safely deliver therapeutic genes to target cells and achieve stable expression. However, gene delivery faces many challenges [18]. Inefficient gene delivery and limitations in targeting can lead to expression of genes in non-target tissues, compromising therapeutic efficacy and increasing side effects [19]. For central nervous system diseases, gene delivery systems need to cross the blood-brain barrier (BBB), which is a challenging task. Therefore, future research must develop more efficient and safer delivery systems and combine them with emerging technologies, such as gene editing and nanotechnology, to overcome existing bottlenecks and advance the clinical application of gene therapy [20].

Based on the above research, a cell membrane-based encapsulated nanobionic particle was designed here for the treatment of glioma by synergizing phototherapy with gene therapy. First, the extraction of cell membrane was achieved by culturing U87 cells (human brain astrocytoblastoma cells) in large quantities and extracting their cell membranes; the large amount of biological information present on the surface of cell membranes gives them a homologous targeting effect, and thus the cell membrane mimicry strategy enhances the uptake of nanomaterials by cells, which has the potential to penetrate the BBB. Furthermore, silver nanoparticles (Ag NPs) were used as templates to synthesize gold nanoparticles (Au NPs) with absorption in the NIR region as carriers. The gold nanoparticles were functionalized with Bcl-2 siRNA and modified into Bcl-2@Au NPs-CM by binding to extracted tumor cell membranes. The functionalized Bcl-2@Au NPs-CM was designed to

DOI: 10.54254/2753-8818/99/2025.23533

target the tumor region and enter the cancer cells. After Bcl-2@Au NPs-CM enters the cell, Bcl-2@Au NPs are released after cell membrane fusion, and the nanoparticles generate heat under 808 nm laser irradiation, which destroys the cancer cells and leads to apoptosis of the tumor cells. The Bcl-2 siRNA carried by Bcl-2@Au NPs can target molecules of specific mRNAs and prevent the synthesis of target proteins through RNA interference (RNAi) technology. As an apoptosis-inhibiting protein, the inhibition of Bcl-2 function enhances the PTT effect and thus accelerates the apoptosis of tumor cells. Ultimately, the tumor cells are destroyed and the target mRNA is silenced, preventing the production of relevant proteins and achieving the effect of cancer treatment. The multifunctional application of Bcl-2@Au NPs-CM in tumor therapy combines physical therapy (PTT) and molecular biology techniques (gene silencing) for more effective cancer treatment. Meanwhile, this multifunctional and synergistic treatment provides new insights for clinical glioma treatment.

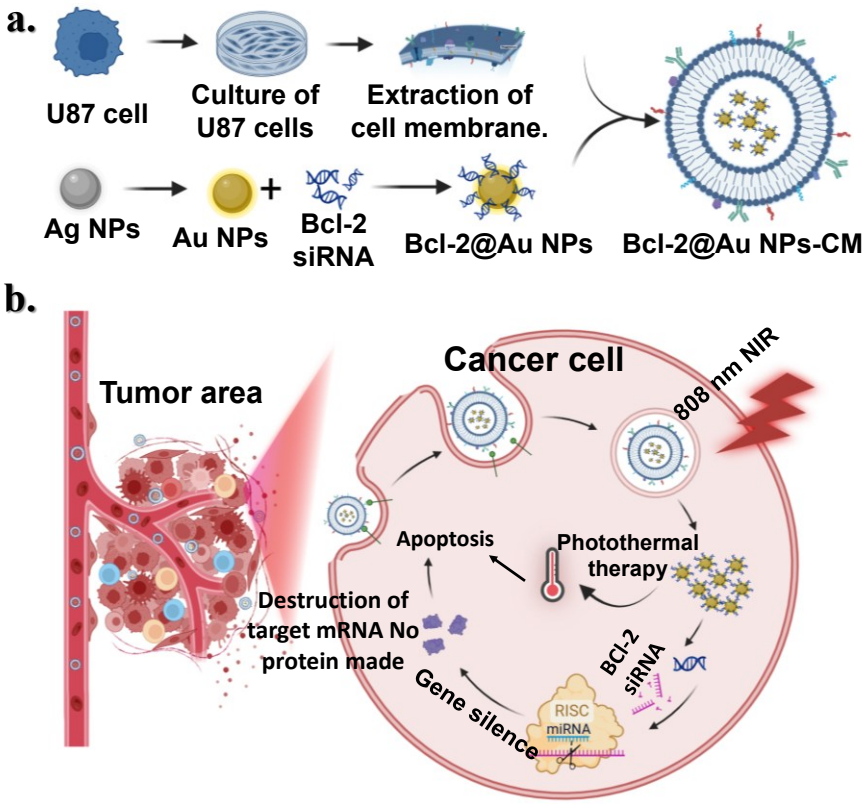

Scheme 1: Schematic diagram of nanomimetic Bcl-2@Au NPs-CM for the treatment of glioma. a. Formation of Bcl-2@Au NPs-CM; b. Antitumor effects of Bcl-2@Au NPs-CM

2. Materials and methods

2.1. Chemistry

Silver nitrate ($AgNO_3$), povidone iodine (PVP), Polyethylene glycol (EG) and $HAuCl_4 \cdot 3H_2O$ sodium sulfide ($Na_2S \cdot 9H_2O$, 99%) were purchased from Sigma-Aldrich.

2.2. Formation of Au nanoparticles (Au NPs)

The starting process is the synthesis of the gold nanoparticles, which is the Au NPs. The Au NPs, is synthesized from the Ag Templates. To prepare the Ag Templates, the materials needed are $AgNO_3$, PVP, and EG, via preparing materials, the $AgNO_3$ and PVP are dissolved in the ethylene glycol,

DOI: 10.54254/2753-8818/99/2025.23533

where the solution is heated to 90 ℃, in a time range of 6 h. Galvanic replacement would utilize to form the Au NPs. The materials which are needed are PVP solution in water, which are freshly prepared with $HAuCl_4$, the Ag should be dispersed in the PVP solution. Thus, $HAuCl_4$ is added dropwise. During which, the localized surface plasmon resonance peak should be monitored by UV-Vis Spectroscopy. The addition is complete once the peak reaches the 808 nm light beam.

2.3. Completion of Bcl-2 siRNA functionalization modification on Au NPs (Bcl-2@Au NPs)

Once the gold nanoparticles are successfully synthesized, the Bcl-2 siRNA was integrated to enhance the ability of gene-silencing. Separated samples of Au NPs were incubated overnight with a Bcl-2 siRNA solution under a stirring at 27 ℃. The electrostatic interactions between the siRNA negatively charged phosphate backbone and the same for the nanoparticle surface can complete stable loading. (some transfection agents could be introduced to enhance adsorption) Via incubation, a centrifuge would take place to pellet the siRNA coated particles. UV-Vis spectrophotometer was used to measure absorbance at 260 nm in the supernatant (For calculations of loading efficiency: compare the absorbance to standard curve for known siRNA concentrations.)

2.4. Tumor cell membrane encapsulation of Bcl-2@Au NPs (Bcl-2@Au NPs-CM)

Cell Culture and Harvesting: Culture tumor cells in a T-75 flask using appropriate cell culture medium at 37°C in a 5% CO_2 incubator until they reach 80-90% confluency. Wash the cells twice with PBS to remove residual medium and serum. Detach the cells using 2-3 mL of trypsin-EDTA solution and incubate at 37°C for 3-5 min. Neutralize the trypsin with 5 mL of complete medium and collect the cell suspension in a 50 mL centrifuge tube. Centrifuge the cell suspension at 1,000 rpm for 5 min to pellet the cells. Discard the supernatant and resuspend the cell pellet in 10 mL of PBS.

Isolation of Tumor Cell Membranes: Resuspend the cell pellet in 5 mL of hypotonic lysis buffer and incubate on ice for 30 minutes to allow cell swelling. Homogenize the cell suspension using a Dounce homogenizer (30-40 strokes) to lyse the cells and release the cell membranes. Centrifuge the lysate at 3,000 rpm for 10 min at 4°C to remove unbroken cells and nuclei. Collect the supernatant and centrifuge at 20,000 rpm for 30 min at 4°C to pellet the cell membranes. Wash the membrane pellet twice with PBS and resuspend in 1 mL of PBS.

Encapsulation of Bcl-2@Au NPs with Tumor Cell Membranes: Mix the Bcl-2@Au NPs solution (1 mg/mL) with the isolated tumor cell membranes at a 1:10 weight ratio (Bcl-2@Au NPs: cell membrane protein). Pass the mixture through a syringe extruder equipped with a 200 nm polycarbonate membrane 10-15 times to ensure uniform encapsulation of the nanoparticles by the cell membranes. Centrifuge the extruded mixture at 20,000 rpm for 30 min at 4°C to remove unbound cell membrane fragments. Resuspend the pellet in PBS to obtain the final Bcl-2@Au NPs-CM formulation.

Measure the hydrodynamic diameter and zeta potential of Bcl-2@Au NPs-CM using dynamic light scattering (DLS) and zeta potential analyzer. Confirm the successful encapsulation of Bcl-2@Au NPs by tumor cell membranes using transmission electron microscopy (TEM).

2.5. Photothermal performance testing of Bcl-2@Au NPs-CM

Dilute the Au NPs、Bcl-2@Au NPs and Bcl-2@Au NPs-CM suspension to a concentration of 100 μg/mL in PBS. Aliquot 1 mL of the Au NPs、Bcl-2@Au NPs and Bcl-2@Au NPs-CM suspension and PBS control into separate wells quartz cuvettes. Calibrate the NIR laser to ensure a stable output power of 0.75 W/cm² at 808 nm wavelength. Use a laser power meter to verify the power density before the experiment. Position the laser source at a fixed distance from the sample to ensure uniform

DOI: 10.54254/2753-8818/99/2025.23533

illumination. Photothermal Heating Experiment: Place the cuvette containing the samples on a stable surface. Insert a thermocouple probe into the sample or use an infrared thermal imaging camera to monitor the temperature changes in real-time. Turn on the NIR laser and irradiate the samples for 10 minutes and record temperature changes.

2.6. Biosafety and tumor killing assay of Bcl-2@Au NPs-CM

Seed tumor cells in a 96-well plate at a density of 5,000 cells per well in 100 μL of complete medium. Incubate the plate at 37°C in a 5% CO_2 incubator for 24 h to allow cell attachment. Prepare serial dilutions of Au NPs, Bcl-2@Au NPs, and Bcl-2@Au NPs-CM in complete medium (100 μg/mL). Treat the cells with Au NPs, Bcl-2@Au NPs, and Bcl-2@Au NPs-CM (100 μg/mL) for 6 h to allow cellular uptake. For the NIR irradiation group, expose the cells to an 808 nm NIR laser at a power density of 0.75 W/cm² for 10 min. For the non-irradiation group, keep the cells under the same conditions without laser exposure. After irradiation, replace the PBS with complete medium and incubate the cells for an additional 24 h. Add 10 μL of CCK-8 reagent to each well and incubate for 1-4 h at 37°C. Perform the CCK-8 assay as described above to quantify cell viability. Incubate the plate at 37 °C in a 5% CO_2 incubator for 24 h. Calculate cell viability as a percentage relative to the PBS control.

2.7. siRNA release ability assay of Bcl-2@Au NPs-CM

Transfer 1 mL of Bcl-2@Au NPs and Bcl-2@Au NPs-CM suspension (100 μg/mL) into a dialysis bag (MWCO: 10 kDa). Place the dialysis bag in a beaker containing 50 mL of PBS (pH 7.4) to simulate physiological conditions. Incubate the setup at 37°C with gentle shaking (100 rpm). At predetermined time points (e.g., 0, 1, 6, 12, 24, 48, 72 h), collect 1 mL of the external PBS solution and replace it with fresh PBS. The release rate of siRNA was calculated by measuring its absorption value at 260 nm.

2.8. Tumor targeting ability assay of Bcl-2@Au NPs-CM (24-well plate)

Seed tumor cells in 6-well plates at a density of 1×10^5 cells per well in 2 mL of complete medium. Incubate the plates at 37°C in a 5% CO_2 incubator for 24 h to allow cell attachment. Replace the medium in each well with 2 mL of fresh complete medium containing 100 μg/mL of fAu NPs, Bcl-2@Au NPs, and Bcl-2@Au NPs-CM. Incubate the cells at 37°C in a 5% CO_2 incubator for 6 h to allow cellular uptake. Tumor cells treated with PBS (negative control). After 6 h, cells from different groups of treatments were collected. Flow cytometry was used to detect the material taken up by the cells.

2.9. Cell live/dead staining assay

Seed tumor cells in a 24-well plate at a 2×10^4 density of cells per well in 100 μL of complete medium. Incubate the plate at 37°C in a 5% CO_2 incubator for 24 h. Prepare serial dilutions of Au NPs, Bcl-2@Au NPs, and Bcl-2@Au NPs-CM in complete medium (100 μg/mL). Treat the cells with Au NPs, Bcl-2@Au NPs, and Bcl-2@Au NPs-CM (100 μg/mL) for 6 h to allow cellular uptake. For the NIR irradiation group, expose the cells to an 808 nm NIR laser at a power density of 0.75 W/cm² for 10 min. For the non-irradiation group, keep the cells under the same conditions without laser exposure. After irradiation incubate the cells for an additional 18 h. Add Calsine and PI reagent to each well and incubate for 10 min h at 37°C. Photographs were subsequently imaged using a laser confocal microscope.

DOI: 10.54254/2753-8818/99/2025.23533

2.10. Gene silencing efficiency assay

Seed tumor cells in 6-well plates at a density of 1×10^5 cells per well in 2 mL of complete medium. Incubate the plates at 37°C in a 5% CO_2 incubator for 24 h. Treat the cells with the following: 、Au NPs、Bcl-2@Au NPs and Bcl-2@Au NPs-CM (100 μg/mL), and incubate the cells at 37°C in a 5% CO_2 incubator for 24 h to allow gene silencing. At the end of the incubation collect the cells to extract RNA and reverse transcribe the RNA into cDNA. Include technical replicates for each sample to ensure reproducibility. Finally, qPCR was utilized to verify the gene silencing efficiency of Bcl-2 siRNA.

Primer Design:

Bcl-2 siRNA forward: 5′-GCUUGAAAUCUAUGCACUCdTdT-3’

Bcl-2 siRNA reverse: 5′-AUGAGUGCAUAGAUUUCAAdTdT-3’.

2.11. Cell proliferation ability assay

Seed tumor cells in a 24-well plate at a density of 2×10^4 cells per well in 500 μL of complete medium. Incubate the plate at 37°C in a 5% CO_2 incubator overnight to allow cell attachment and growth. Dilute Au NPs, Bcl-2@Au NPs, and Bcl-2@Au NPs-CM to a final concentration of 100 μg/mL in complete medium. Replace the medium in each well with 500 μL of the nanoparticle suspensions or PBS (untreated control). Incubate the plate at 37°C in a 5% CO_2 incubator for 24 h to allow cellular uptake and treatment. Prepare the EDU working solution according to the manufacturer’s instructions, incubate the plate at room temperature for 3 h in the dark. Add 500 μL of Hoechst 33342 (1 μg/mL) to each well for nuclear staining. Imaging analysis using laser confocal microscopy.

3. Results and discussion

3.1. Characterization of Au NPs and Bcl-2@Au NPs-CM

The morphological and structural characteristics of the synthesized gold nanoparticles (Au NPs) and cell membrane-coated Bcl-2@Au NPs (Bcl-2@Au NPs-CM) were investigated using transmission electron microscopy (TEM). As shown in **Figure 1**, the left panel displays the TEM image of bare Au NPs **(Figure 1a)**, which exhibit a uniform spherical morphology with an average diameter of approximately 20 nm. The high contrast observed in the TEM image confirms the successful synthesis of AuNPs with well-defined size distribution and crystallinity. In the right panel of **Figure 1**, the TEM image reveals the successful coating of Bcl-2@Au NPs with a cell membrane (Bcl-2@Au NPs-CM) **(Figure 1b)**. The cell membrane-coated AuNPs exhibit a core-shell structure, where the dark core corresponds to the AuNPs, and the lighter surrounding layer represents the cell membrane. The average size of the cell membrane-coated Au NPs is approximately 200 nm, indicating a significant increase in size compared to the bare AuNPs. This size increase is attributed to the Encapsulates multiple Au NPs. The successful coating of AuNPs with cell membranes is further supported by the distinct boundary observed between the core and the shell in the TEM image. This core-shell structure is crucial for the functionalization of Au NPs, as the cell membrane coating can provide biomimetic properties, such as immune evasion and targeted delivery, which are essential for biomedical applications, particularly in cancer therapy. The TEM results demonstrate the successful synthesis and functionalization of Au NPs with cell membranes. The uniform size and morphology of the bare AuNPs are critical for their optical and electronic properties, which are highly dependent on particle size and shape. The cell membrane coating not only enhances the biocompatibility of AuNPs but also endows them with unique biological functionalities. For instance, the cell membrane can provide

DOI: 10.54254/2753-8818/99/2025.23533

homotypic targeting capabilities, enabling the Au NPs to specifically recognize and bind to cancer cells.

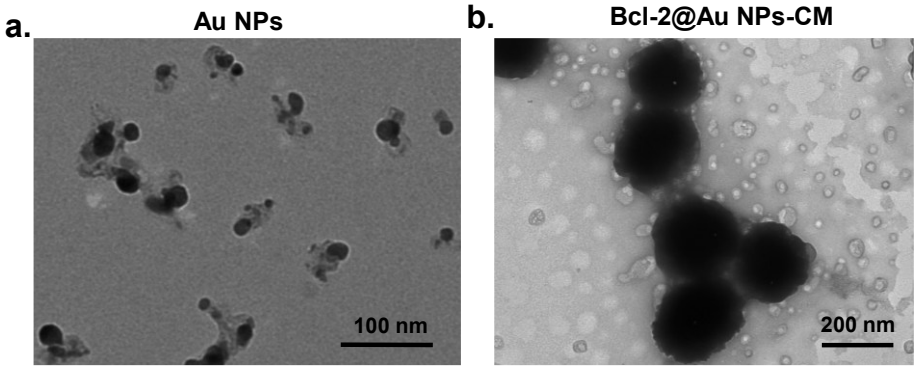

Figure 1: **TEM images.** a. TEM images of Au NPs; b. TEM images of Bcl-2@Au NPs-CM

The absorption curves of both Ag NPs and Au NPs were further determined. From the experimental results **(Figure 2)**, the synthesis of Au NPs using Ag NPs as a template has localized the localized surface plasmon resonance (LSPR) properties to extend into the near infrared region.808 The increase in absorption in the nano band is very advantageous for photothermal applications, allowing deeper penetration into tissues and minimizing damage to the surrounding healthy tissues.808 The increase in absorption in the nano band makes Au NPs an ideal candidate for photothermal therapeutics. makes Au NPs an ideal candidate for photothermal therapeutics. When exposed to near-infrared laser light at this wavelength, Au NPs efficiently convert light energy into thermal energy, resulting in localized heating and subsequent ablation of tumor cells. This property, coupled with the biocompatibility and stability of gold-based nanomaterials, makes Au NPs an excellent platform for targeted cancer therapy.

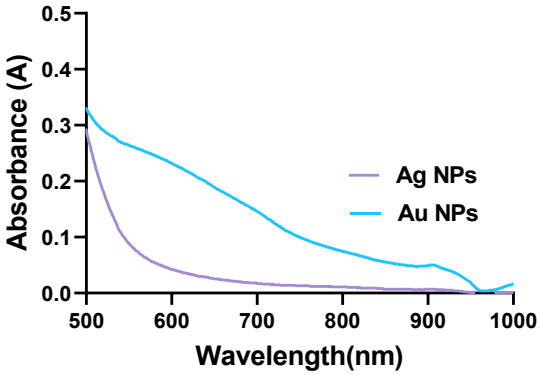

Figure 2: Absorption curves of Ag NPs and Au NPs

The hydrodynamic diameters and zeta potentials of Au NPs, Bcl-2@Au NPs and Bcl-2@Au NPs-CM were characterized to assess the effects of surface modification and cell membrane encapsulation on their physicochemical properties. As shown in **Figure 3a**, the hydrodynamic diameter of the nanoparticles gradually increased with each step of modification. The bare gold NPs had the smallest size, which is consistent with their well-defined synthesis process. After conjugation with Bcl-2 siRNA, the diameter of the Bcl-2@Au NPs increased to approximately 200 nm, which may be due to the presence of an siRNA layer on the surface of the nanoparticles. After further encapsulation with tumor cell membranes, the size of Bcl-2@Au NPs-CMs increased significantly with an average diameter of about 280 nm. This increase in size indicated the successful formation of a core-shell

DOI: 10.54254/2753-8818/99/2025.23533

structure, with the cell membrane forming a thick outer layer around the nanoparticle core. The gradual increase in size confirms the process of progressive modification and encapsulation, which is essential to ensure the functionalization and biocompatibility of the nanoparticles. As shown in **Figure 3b**, zeta potential measurements show a corresponding trend in the surface charge of the nanoparticles. The bare Au NPs have the highest zeta potential and are strongly negatively charged due to the presence of stabilizers on their surface. Conjugation with Bcl-2 siRNA lowered the zeta potential of Bcl-2@Au NPs because the negatively charged siRNA molecules partially neutralized the surface charge. Encapsulation of Bcl-2@Au NPs with tumor cell membranes further reduced the zeta potential of Bcl-2@Au NPs-CM, bringing its surface charge close to neutral. The reduction in zeta potential was consistent with the presence of cell membranes, which mimic the natural surface properties of biological cells, enhancing the biocompatibility and invisibility of the nanoparticles.

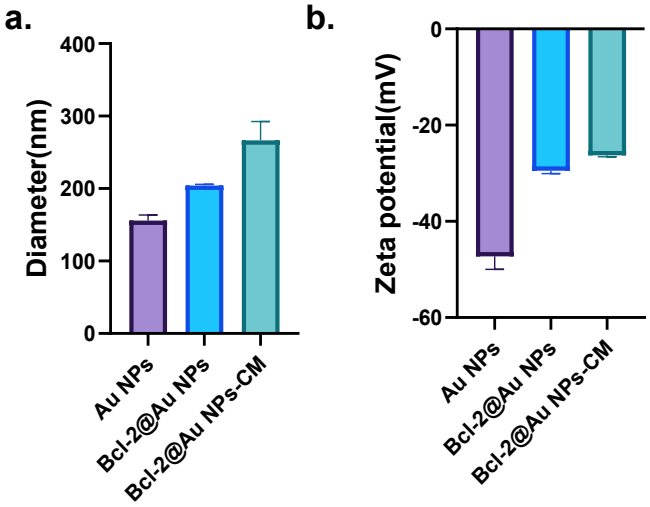

Figure 3: a. Plot of particle size results, b. Plot of potential results

3.2. Performance research

The siRNA release profiles of Bcl-2@Au NPs and Bcl-2@Au NPs-CM were evaluated over a period of 72 h to assess the impact of cell membrane encapsulation on the release kinetics. As shown in **Figure 4a**, the cumulative siRNA release from Bcl-2@Au NPs reached approximately 60% within 72 h, demonstrating a relatively rapid release profile. In contrast, Bcl-2@Au NPs-CM exhibited a slower release rate, with only about 50% of the siRNA released over the same period. This difference in release efficiency highlights the significant role of the cell membrane encapsulation in modulating the siRNA release kinetics. The slower release observed for Bcl-2@Au NPs-CM can be attributed to the physical barrier provided by the cell membrane, which acts as a protective layer around the nanoparticle core. This barrier not only delays the diffusion of siRNA molecules but also provides a more controlled and sustained release profile. The sustained release mechanism is particularly advantageous for therapeutic applications, as it ensures a prolonged and consistent delivery of siRNA to the target cells, thereby enhancing the efficacy of gene silencing.

The photothermal performance of Au NPs, Bcl-2@Au NPs, and Bcl-2@Au NPs-CM was evaluated under 808 nm laser irradiation over a 10 min period **(Figure 4b)**. All three nanostructures demonstrated a significant temperature increase, reaching the threshold required for effective photothermal therapy. Notably, Bcl-2@Au NPs-CM exhibited a slightly lower maximum temperature (49°C) compared to the other formulations. Despite this minor reduction, the temperature achieved by Bcl-2@Au NPs-CM remains sufficient to induce apoptosis in tumor cells, highlighting its potential for effective photothermal tumor ablation. The slight decrease in temperature may be attributed to the

DOI: 10.54254/2753-8818/99/2025.23533

insulating effect of the cell membrane coating, which could influence heat transfer dynamics. These findings suggest that Bcl-2@Au NPs-CM retains its therapeutic capability while potentially benefiting from the biomimetic properties conferred by the cell membrane.

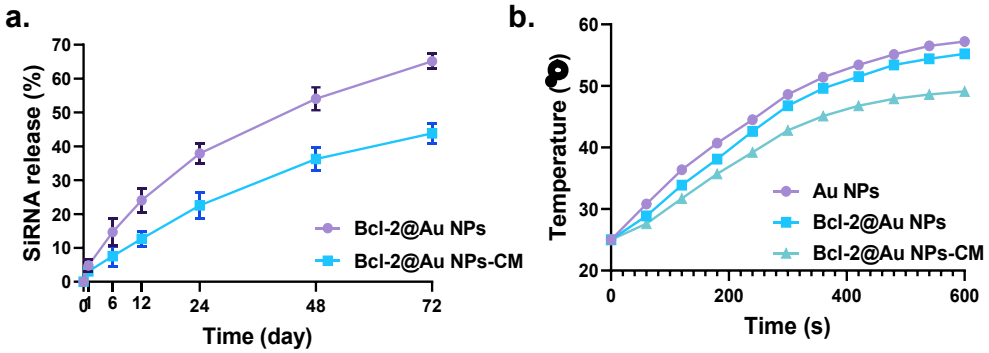

Figure 4: **Performance characterization.** a. siRNA release ability test; b. Photothermal performance test

3.3. Biological targeting and tumor killing capability

Figure 5a illustrates the cellular targeting capabilities of Au NPs, Bcl-2@Au NPs, and Bcl-2@Au NPs-CM as determined by flow cytometry analysis. While both Au NPs and Bcl-2@Au NPs exhibited moderate targeting ability compared to the control group, Bcl-2@Au NPs-CM demonstrated the strongest targeting efficiency. This enhanced targeting effect can be attributed to the homotypic binding properties conferred by the cell membrane coating, which promotes selective recognition and adhesion to tumor cells of the same origin. These results underscore the advantage of cell membrane-coated nanoparticles in enhancing tumor-specific delivery and improving therapeutic outcomes.

Figure 5b presents the effect of Au NPs, Bcl-2@Au NPs, and Bcl-2@Au NPs-CM on tumor cell viability, as evaluated using the CCK-8 assay. In the absence of light irradiation, none of the three materials caused a significant reduction in cell viability, indicating good biocompatibility. Notably, Bcl-2@Au NPs-CM further improved cell viability, likely due to the protective properties conferred by the cell membrane coating. However, under 808 nm near-infrared (NIR) laser irradiation, Bcl-2@Au NPs-CM induced significant tumor cell death. This enhanced cytotoxicity is attributed to the synergistic effect of photothermal therapy and gene modulation, underscoring the therapeutic potential of Bcl-2@Au NPs-CM for targeted tumor treatment.

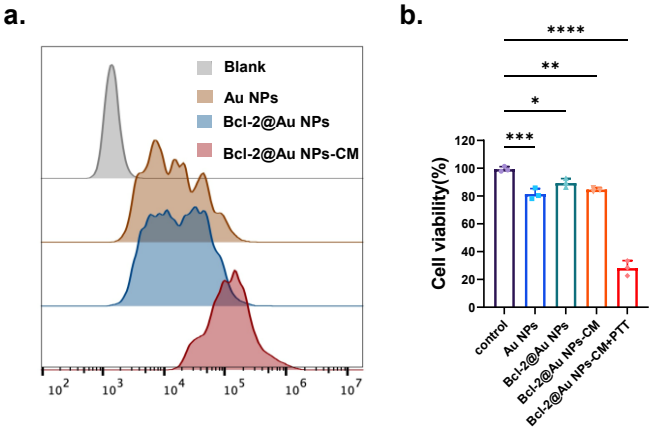

Figure 5: a. Detection of the targeting ability of each group of materials on tumor cells using flow cytometry. b. Cell activity test

DOI: 10.54254/2753-8818/99/2025.23533

3.4. Gene silencing

The gene silencing efficiency of Bcl-2 siRNA delivered by Au NPs, Bcl-2@Au NPs, and Bcl-2@Au NPs-CM was evaluated using quantitative polymerase chain reaction (qPCR) to measure the relative expression levels of Bcl-2 mRNA. As shown in **Figure 6**, the results demonstrate that Bcl-2@Au NPs-CM exhibited the most potent gene silencing effect, achieving an 80% reduction in Bcl-2 mRNA expression compared to the untreated control. This remarkable silencing efficiency significantly outperformed both bare Au NPs and Bcl-2@Au NPs, which showed only marginal or moderate reductions in Bcl-2 mRNA levels, respectively. The superior gene silencing performance of Bcl-2@Au NPs-CM can be attributed to two key factors: its enhanced tumor-targeting ability and the effective release of Bcl-2 siRNA. As demonstrated in previous targeting assays, the cell membrane encapsulation of Bcl-2@Au NPs-CM enables homotypic targeting, allowing the nanoparticles to specifically recognize and bind to tumor cells. This targeted delivery ensures a higher accumulation of nanoparticles at the tumor site, thereby increasing the local concentration of siRNA and enhancing its therapeutic effect. Additionally, the controlled and sustained release of siRNA from Bcl-2@Au NPs-CM, as evidenced by the siRNA release assay, ensures a prolonged and efficient delivery of siRNA into the target cells, further contributing to the robust gene silencing observed. The combination of these factors—targeted delivery and effective siRNA release—enables Bcl-2@Au NPs-CM to achieve a significant downregulation of Bcl-2 mRNA expression. Bcl-2 is a critical anti-apoptotic protein, and its suppression can sensitize tumor cells to apoptosis, making it a promising therapeutic strategy for cancer treatment.

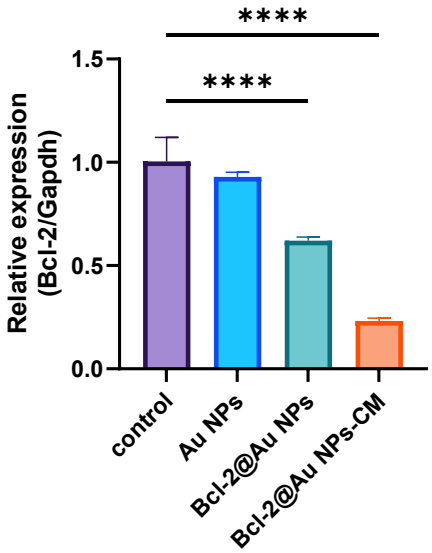

Figure 6: Bcl-2 mRNA expression was detected by qPCR

3.5. Proliferation of tumor cells by Bcl-2@Au NPs-CM

Figure 7 illustrates the live/dead staining results of tumor cells treated with Au NPs, Bcl-2@Au NPs, Bcl-2@Au NPs-CM, and Bcl-2@Au NPs-CM combined with PTT. In the absence of light exposure, cells across all treatment groups remained intact, showing predominantly green fluorescence, indicative of live cells. However, after the introduction of PTT, a significant reduction in cell number was observed, accompanied by morphological changes such as cell rounding and an increase in red fluorescence, signifying cell death. These findings demonstrate that the Bcl-2@Au NPs-CM + PTT treatment induces higher levels of tumor cell death, highlighting its potent tumor-killing efficacy.

DOI: 10.54254/2753-8818/99/2025.23533

This enhanced therapeutic effect can be attributed to the synergistic action of photothermal and gene therapy, effectively amplifying the treatment outcome.

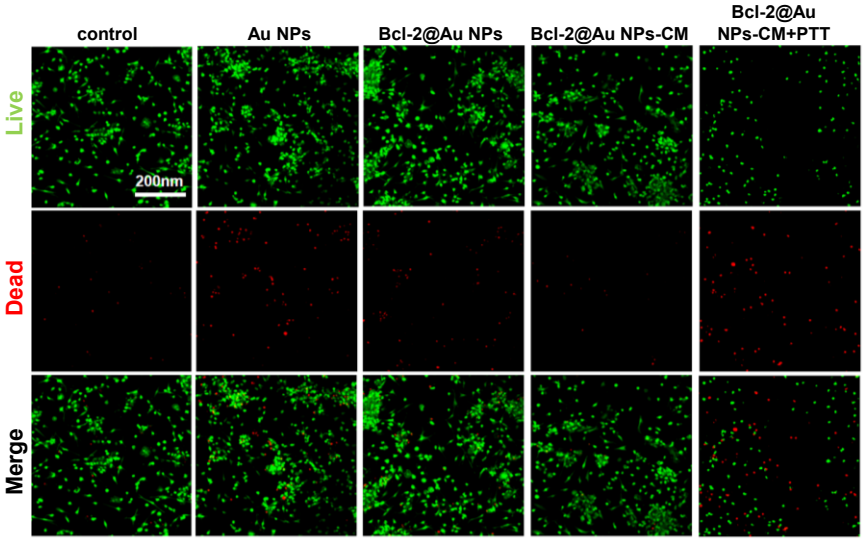

Figure 7: Cell live/dead staining

Figure 8 presents the results of cell proliferation assays using the EDU-488 kit to evaluate the effects of Au NPs, Bcl-2@Au NPs, and Bcl-2@Au NPs-CM on tumor cell proliferation. The experimental results indicate that tumor cells treated with Bcl-2@Au NPs-CM exhibited the weakest green fluorescence, suggesting the lowest level of cell proliferation. This observation demonstrates that Bcl-2@Au NPs-CM effectively inhibits tumor cell growth and reproduction, highlighting its superior anti-tumor potential. These findings underscore the therapeutic promise of Bcl-2@Au NPs-CM in combating tumor progression by targeting cellular proliferation pathways.

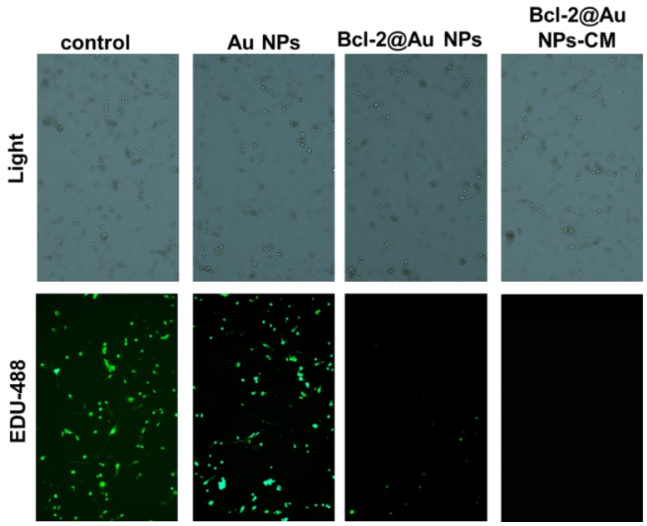

Figure 8: Imaging diagram of EDU-488 cell proliferation assay

4. Conclusion

1. In terms of materials, Au nanoparticles with near-infrared light absorption were successfully synthesized by using Ag as a template to synthesize well-dispersed Au NPs with absorption in the near-infrared region.

DOI: 10.54254/2753-8818/99/2025.23533

2. Bcl-2@Au NPs-CM can target the tumor region, while Bcl-2@Au NPs-CM has good biosafety in the absence of light.

3. Under the near-infrared illumination of 808 nm, the material has good photothermal properties, and the temperature can reach 49°C and kill tumor cells.

4. Bcl-2@Au-CM NPs have the ability of slow-release siRNA, with higher delivery efficiency in the tumor region, while silencing BCl-2 siRNA, enhancing apoptosis and inhibiting tumor cell proliferation

References

[1] *C. Grady, K. Melnick, K. Porche, F. Dastmalchi, D. J. Hoh, M. Rahman and A. Ghiaseddin. Glioma Immunotherapy: Advances and Challenges for Spinal Cord Gliomas. Neurospine 2022, 19, 1, 13-29.*

[2] *L. Xiong, F. Wang and X. Q. Xie. Advanced treatment in high-grade gliomas. Journal of Buon 2019, 24, 2, 424-430.*

[3] *A. M. Giantini-Larsen, A. Pandey, A. L. A. Garton, M. Rampichini, G. Winston, J. L. Goldberg, R. Magge, P. E. Stieg, M. M. Souweidane and R. Ramakrishna. Therapeutic manipulation and bypass of the blood-brain barrier: powerful tools in glioma treatment. Neuro-oncology advances 2025, 7, 1, vdae201-vdae201.*

[4] *E. Belykh, K. V. Shaffer, C. Lin, V. A. Byvaltsev, M. C. Preul and L. Chen. Blood-Brain Barrier, Blood-Brain Tumor Barrier, and Fluorescence-Guided Neurosurgical Oncology: Delivering Optical Labels to Brain Tumors. Frontiers in Oncology 2020, 10,*

[5] *W. Stummer and M. A. Kamp. The importance of surgical resection in malignant glioma. Current Opinion in Neurology 2009, 22, 6, 645-649.*

[6] *S. Choi, Y. Yu, M. R. Grimmer, M. Wahl, S. M. Chang and J. F. Costello. Temozolomide-associated hypermutation in gliomas. Neuro-Oncology 2018, 20, 10, 1300-1309.*

[7] *T. Mesti and J. Ocvirk. Malignant gliomas: old and new systemic treatment approaches. Radiology and Oncology 2016, 50, 2, 129-138.*

[8] *H. S. Han and K. Y. Choi. Advances in Nanomaterial-Mediated Photothermal Cancer Therapies: Toward Clinical Applications. Biomedicines 2021, 9, 3.*

[9] *D. An, J. Fu, B. Zhang, N. Xie, G. Nie, H. Agren, M. Qiu and H. Zhang. NIR-II Responsive Inorganic 2D Nanomaterials for Cancer Photothermal Therapy: Recent Advances and Future Challenges. Advanced Functional Materials 2021, 31, 32.*

[10] *M. Debnath, S. K. Debnath, M. V. Talpade, S. Bhatt, P. P. Gupta and R. Srivastava. Surface engineered nanohybrids in plasmonic photothermal therapy for cancer: Regulatory and translational challenges. Nanotheranostics 2024, 8, 2, 202-218.*

[11] *A. S. C. Goncalves, C. F. Rodrigues, A. F. Moreira and I. J. Correia. Strategies to improve the photothermal capacity of gold-based nanomedicines. Acta Biomaterialia 2020, 116, 105-137.*

[12] *N. Gupta and R. Malviya. Understanding and advancement in gold nanoparticle targeted photothermal therapy of cancer. Biochimica Et Biophysica Acta-Reviews on Cancer 2021, 1875, 2,*

[13] *S. Yu, G. Xia, N. Yang, L. Yuan, J. Li, Q. Wang, D. Li, L. Ding, Z. Fan and J. Li. Noble Metal Nanoparticle-Based Photothermal Therapy: Development and Application in Effective Cancer Therapy. International Journal of Molecular Sciences 2024, 25, 11,*

[14] *J. Kim, J. Kim, C. Jeong and W. J. Kim. Synergistic nanomedicine by combined gene and photothermal therapy. Advanced Drug Delivery Reviews 2016, 98, 99-112.*

[15] *L. Qin, S. Jiang, H. He, G. Ling and P. Zhang. Functional black phosphorus nanosheets for cancer therapy. Journal of Controlled Release 2020, 318, 50-66.*

[16] *F. Arabi, V. Mansouri and N. Ahmadbeigi. Gene therapy clinical trials, where do we go? An overview. Biomedicine & Pharmacotherapy 2022, 153.*

[17] *B. Cesur-Erguen and D. Demir-Dora. Gene therapy in cancer. Journal of Gene Medicine 2023, 25, 11.*

[18] *R. E. MacLaren, J. Bennett and S. D. Schwartz. Gene Therapy and Stem Cell Transplantation in Retinal Disease: The New Frontier. Ophthalmology 2016, 123, 10, S98-S106.*

[19] *A. Regenauer. Gene Therapy for Cancer - A New Dimension and Challenge for Insurers. Journal of insurance medicine (New York, N.Y.) 2019, 48, 1, 58-64.*

[20] *Y. Yao and F. Bei. Adeno-associated Virus-Mediated Gene Delivery Across the Blood-Brain Barrier. Advances in neurobiology 2024, 41, 91-112.*